

Electron-Transfer Salts of 1,2,3,4,5-Pentamethylferrocene, $\text{Fe}^{\text{II}}(\text{C}_5\text{Me}_5)(\text{C}_5\text{H}_5)$. Structure and Magnetic Properties of Two 1:1 and Two 2:3 $\text{Fe}(\text{C}_5\text{Me}_5)(\text{C}_5\text{H}_5)$ Electron-Transfer Salts of Tetracyanoethylene

Joel S. Miller,^{*,1a,b} Daniel T. Glatzhofer,^{1b-d} Carlos Vazquez,^{1b} R. Scott McLean,^{1b}
Joseph C. Calabrese,^{1b} Will J. Marshall,^{1b} and James W. Raebiger^{1a}

Department of Chemistry, University of Utah, Salt Lake City, Utah 84112-0850, Central Research and Development, Du Pont, Experimental Station E328, Wilmington, Delaware 19880-0328, and Department of Physics, The Ohio State University, Columbus, Ohio 43210-1106

Received December 12, 2000

The reaction of $\text{Fe}^{\text{II}}(\text{C}_5\text{Me}_5)(\text{C}_5\text{H}_5)$, FeCpCp^* , with percyano acceptors, A [$\text{A} = \text{C}_4(\text{CN})_6$ (hexacyanobutadiene), TCNQF_4 (perfluoro-7,7,8,8-tetracyano-*p*-quinodimethane), and DDQ (2,3-dichloro-5,6-dicyanobenzoquinone)], results in formation of 1:1 charge-transfer salts of $[\text{Fe}^{\text{III}}\text{CpCp}^*]^+[\text{A}]^-$ composition. With $\text{A} = \text{TCNQ}$ (7,7,8,8-tetracyano-*p*-quinodimethane) a 1:2 electron-transfer salt with FeCpCp^* forms. With $\text{A} = \text{TCNE}$ (tetracyanoethylene) a pair of 1:1 salts as well as a pair of 2:3 salts of $[\text{FeCpCp}^*]_2[\text{TCNE}]_3 \cdot \text{S}$ ($\text{S} = \text{CH}_2\text{Cl}_2$, THF) have been isolated and characterized by single-crystal X-ray diffraction. $[\text{FeCpCp}^*][\text{TCNE}]$ consists of parallel 1-D $\cdots\text{D}^+\text{A}^-\text{D}^+\text{A}^-\text{D}^+\text{A}^-\cdots$ chains, while $[\text{FeCpCp}^*]_2[\text{TCNE}]_3 \cdot \text{MeCN}$ has a herringbone array of $\text{D}^+\text{A}_2^-\text{D}^+$ dimers separated by solvent molecules. Although each $[\text{TCNE}]^-$ is disordered, the diamagnetic $[\text{TCNE}]_2^{2-}$ dimer is structurally different from those observed earlier with an intradimer separation of 2.79 Å. The $[\text{TCNE}]^-$ in the 2:3 $[\text{FeCpCp}^*]_2[\text{TCNE}]_3 \cdot \text{S}$ exists as an eclipsed diamagnetic $[\text{TCNE}]_2^{2-}$ dimer with an intradimer ethylene $\text{C}\cdots\text{C}$ separation of 2.833 and 2.903 Å for the CH_2Cl_2 - and THF-containing materials, respectively. The bond distances and angles for all the cations are essentially equivalent, and the distances are essentially equivalent to those previously reported for $[\text{FeCp}^*_2]^{2+}$ and $[\text{FeCp}_2]^{2+}$ cations. The average $\text{Fe}-\text{C}_5\text{H}_5$ -ring and $\text{Fe}-\text{C}_5\text{Me}_5$ -ring centroid distances are 1.71 and 1.69 Å, respectively, which are 0.05 Å longer than reported for $\text{Fe}^{\text{II}}\text{CpCp}^*$. The one-electron reduction potential for $\text{Fe}^{\text{II}}\text{CpCp}^*$ is 0.11 V (vs SCE). The 5 K EPR of $[\text{FeCpCp}^*]^+[\text{BF}_4]^-$ exhibits an axially symmetric powder pattern with $g_{\parallel} = 4.36$ and $g_{\perp} = 1.24$, and the EPR parameters are essentially identical to those reported for ferrocenium and decamethylferrocenium. The high-temperature magnetic susceptibility for polycrystalline samples of these complexes can be fit by the Curie–Weiss law, $\chi = C/(T - \theta)$, with low θ values and μ_{eff} values from 2.08 to 3.43 μ_{B} , suggesting that the polycrystalline samples measured had varying degrees of orientation. $[\text{FeCpCp}^*][\text{TCNE}]$ exhibits the highest effective moment of 3.43 μ_{B}/Fe and weak ferromagnetic coupling, as evidenced from the θ of 3.3 K; however, unexpectedly, it does not magnetically order above 2 K. The formation of the four phases comprising FeCpCp^* and TCNE emphasizes the diversity of materials that may form and the present inability to predict neither solid-state compositions nor structure types.

Introduction

Bulk ferromagnetic behavior has been observed for the electron-transfer salt of decamethylferrocene, FeCp^*_2 ($\text{Cp}^* =$ pentamethylcyclopentadienide) and tetracyanoethylene, TCNE.^{2,3} In contrast, the similarly structured [i.e., alternating donor/acceptor ($\cdots\text{D}^+\text{A}^-\text{D}^+\text{A}^-\cdots$) ($\text{D} = \text{FeCp}^*_2$, $\text{A} = \text{TCNE}$) 1-D chain] ferrocene charge-transfer complex⁴ $[\text{FeCp}_2][\text{TCNE}]$ is diamagnetic.^{2,4} This difference is due to the ability of FeCp^*_2 ($E^\circ = -0.12$ V vs SCE), unlike FeCp_2 ($E^\circ = 0.41$ V), to reduce

TCNE ($E^\circ = 0.15$ V)⁵ to form an electron-transfer salt. Similarly, the electron-transfer salt of FeCp^*_2 and TCNQ (7,7,8,8-tetracyano-*p*-quinodimethane) forms two $\cdots\text{D}^+\text{A}^-\text{D}^+\text{A}^-\cdots$ complexes, one of which exhibits field-dependent, metamagnetic switching from an antiferromagnetic to a high-moment behavior^{2,6a} and the other of which orders as a ferromagnet at 3.1 K.^{6c} Thus, a sufficiently strong donor appears to be a necessary, but insufficient, component of a molecular ferromagnet or metamagnet.

An insightful framework to view the stabilization of ferromagnetic coupling in molecular-based donor/acceptor complexes is based on the extended McConnell mechanism.^{2,7} Within this model, the stabilization of ferromagnetic coupling arises from the configurational mixing of a charge-transfer excited state with the ground state. The model predicts that for excitation from a

- (1) (a) University of Utah. (b) Du Pont. (c) The Ohio State University. (d) Current address: Department of Chemistry, University of Oklahoma.
- (2) Miller, J. S.; Epstein, A. J. In *Research Frontiers in Magnetochemistry*; O'Connor, C. J., Ed.; World Scientific: River Edge, NJ, 1993; p 283.
- (3) Miller, J. S.; Epstein, A. J. *Angew. Chem., Int. Ed. Engl.* **1994**, *33*, 385.
- (4) Miller, J. S.; Calabrese, J. C.; Rommelmann, H.; Chittipeddi, S.; Epstein, A. J.; Zhang, J. H.; Reiff, W. M. *J. Am. Chem. Soc.* **1987**, *109*, 769.
- (5) Adman, E.; Rosenblum, M.; Sullivan, S.; Margulis, T. N. *J. Am. Chem. Soc.* **1967**, *89*, 4540. Foxman, B. M. Private communication. Sullivan, B. W.; Foxman, B. M. *Organometallics* **1983**, *2*, 187. Rosenblum, M.; Fish, R. W.; Bennett, C. *J. Am. Chem. Soc.* **1964**, *86*, 5166.

- (5) Ward, M. D. *Electroanal. Chem.* **1989**, *6*, 181.
- (6) (a) Miller, J. S.; Reis, A. H., Jr.; Gerbert, E.; Ritsko, J. J.; Saleneck, W. R.; Kovnat, L.; Cape, T. W.; Van Duyne, R. P. *J. Am. Chem. Soc.* **1979**, *101*, 7111. (b) Miller, J. S.; Zhang, J. H.; Reiff, W. M.; Preston, L. D.; Reis, A. H., Jr.; Gerbert, E.; Extine, E.; Troup, J.; Ward, M. D. *J. Phys. Chem.* **1987**, *91*, 4344. (c) Broderick, W. E.; Eichhorn, D. M.; Liu, X.; Toscano, P. J.; Owens, S. M.; Hoffman, B. M. *J. Am. Chem. Soc.* **1995**, *117*, 3641.

non-half-occupied degenerate HOMO of a donor to an acceptor with a half-filled nondegenerate HOMO, as is the case for $[\text{TCNE}]^{\bullet-}$ and $[\text{TCNQ}]^{\bullet-}$, ferromagnetic coupling may be stabilized. Thus, donors (and/or acceptors) with C_n ($n \geq 3$) symmetry are necessary for degenerate orbitals. Hence, simple substituted ferrocenes will lower the symmetry below C_3 , and on the basis of the aforementioned model, these compounds would be inappropriate components for a molecular ferromagnet. This has been observed for $[\text{Fe}(\text{C}_5\text{Me}_4\text{H})_2]^+[\text{TCNE}]^{\bullet-}$ and $[\text{Fe}(\text{C}_5\text{Me}_4\text{H})_2]^+[\text{TCNQ}]^{\bullet-}$, which have the desired 1-D structural motif.⁸

The 1,2,3,4,5-pentamethylferrocene⁹ donor, FeCpCp^* , however, maintains the 5-fold axis, and its radical cation, like $[\text{FeCp}_2]^+$ and $[\text{FeCp}_2]^+$, should have an ${}^2E_{2g}$ ground state. This expectation and facile oxidation (0.11 V) suggested that electron-transfer salts with TCNE and TCNQ might exhibit cooperative magnetic properties should they have the desired 1-D $\cdots\text{D}^+\text{A}^{\bullet-}\text{D}^+\text{A}^{\bullet-}\cdots$ motif. The smaller size of Cp with respect to Cp* should lead to shorter intra- and interchain separations and hence stronger ferromagnetic coupling and consequently enhanced Weiss constants (θ) and ferromagnetic ordering temperatures (T_c). Herein we report several electron-transfer salts based on FeCpCp^* .

Experimental Section

All reactions were performed in a Vacuum Atmospheres Dri-Box under a nitrogen atmosphere. Elemental analyses were performed by Onieda Research Services, Inc. (Whitesboro, NY). Acetonitrile was distilled for 24 h under nitrogen from CaH_2 twice. Cyclic voltammetry was performed in acetonitrile solution containing 0.1 M $[\text{n-Bu}_4\text{N}][\text{ClO}_4]$ electrolyte in a conventional H-cell with a platinum working electrode and a Ag/AgCl reference electrode. All potentials are reported vs SCE. TCNE (Aldrich) was sublimed prior to use, and TCNQ and DDQ (Aldrich) were recrystallized from MeCN and chloroform, respectively, prior to use. $\text{C}_4(\text{CN})_6$,^{10a} TCNQF_4 ,^{10b} and FeCpCp^* ⁹ were prepared according literature methods.

$[\text{FeCpCp}^*]^+[\text{BF}_4]^-$. A solution of 159 mg of a 52% HBF_4 solution in 5 mL of Et_2O with 53 mg (0.49 mmol) of benzoquinone was added to a stirred solution of 250 mg (0.98 mmol) of FeCpCp^* in 5 mL of diethyl ether. The light-green precipitate that formed was collected by filtration and dissolved in a minimal amount of acetonitrile (ca. 2 mL). Diffusion of diethyl ether into the acetonitrile solution for several days enabled the formation of dark-green crystals. The crystals were filtered, washed with diethyl ether, and dried under reduced pressure to give 290 mg (86%). Anal. Calcd (found) for $\text{C}_{15}\text{H}_{20}\text{FeBF}_4$: C, 52.53 (52.66); H, 5.88 (5.73). The reduction potential determined via cyclic voltammetry in acetonitrile is 0.11 V vs SCE.

$\{[\text{FeCpCp}^*]^+\}_2[\text{TCNE}]_2^{2-}\cdot 2\text{MeCN}$. A solution of FeCpCp^* (64 mg, 0.25 mmol) in 3 mL of MeCN was combined with a solution (32 mg, 0.25 mmol) of TCNE in 1 mL of MeCN. The resultant homogeneous solution was placed in the freezer for 18 h, which yielded 63 mg (60%) of black crystals. Anal. Calcd (found) for $\text{C}_{21}\text{H}_{20}\text{N}_4\text{Fe}$: C, 65.64 (65.23); H, 5.25 (5.39); N, 14.58 (14.09). Infrared (Nujol): $\nu(\text{CN}) = 2163\text{m}$, 2175s , and 2192s cm^{-1} .

$\{[\text{FeCpCp}^*]^+\}_2[\text{TCNE}]_2^{2-}\cdot \text{TCNE}\cdot \text{THF}$. A solution of 1.00 g (3.90 mmol) of FeCpCp^* in 5 mL of THF was combined with a solution of 0.500 g (3.90 mmol) of TCNE in 10 mL of THF. The resultant homogeneous solution was placed in the freezer for several days. The dark block crystals were collected by filtration, washed with THF, and

dried under vacuum. Yield = 800 mg (64%). Anal. Calcd (found) for $\text{C}_{52}\text{H}_{48}\text{Fe}_2\text{N}_{12}\text{O}$: C, 64.47 (64.67), H, 4.99 (5.09); N, 17.35 (17.38). Infrared (Nujol): $\nu(\text{CN}) = 2159\text{m}$, 2173s , 2190m , 2237w , and 2263w cm^{-1} . On one occasion, crystals characterized as $[\text{FeCpCp}^*]^+[\text{TCNE}]^-$ by crystallography were isolated. A solution of 60 mg (0.23 mmol) of FeCpCp^* in 2 mL of THF and a solution of 30 mg (0.23 mmol) of TCNE in 3 mL of THF were combined. The volume was reduced to 3 mL, and ether diffusion produced small black crystals. Infrared (Nujol): $\nu(\text{CN}) = 2142\text{s}$ and 2183m cm^{-1} .

$\{[\text{FeCpCp}^*]^+\}_2[\text{TCNE}]_2^{2-}\cdot \text{TCNE}\cdot \text{CH}_2\text{Cl}_2$. A solution of 200 mg (0.781 mmol) of FeCpCp^* in 10 mL of CH_2Cl_2 was combined with a solution of 100 mg (0.781 mmol) of TCNE in 5 mL of CH_2Cl_2 . The resultant homogeneous solution was placed in the freezer for several days. The black needle crystals were collected by filtration, washed with CH_2Cl_2 , and dried under vacuum. Yield = 107 mg (42%). Infrared (Nujol): $\nu(\text{CN}) = 2160\text{s}$, 2173vs , 2190s , 2238w , and 2265w cm^{-1} .

$[\text{FeCpCp}^*]^+[\text{TCNQF}_4]^-$. The compound was prepared from the reaction of FeCpCp^* (75 mg, 0.293 mmol; 10 mL of MeCN) and TCNQF_4 (81 mg, 0.293 mmol; 10 mL of MeCN) in 71% yield (111 mg) after cooling to -20°C for 18 h. Anal. Calcd (found) for $\text{C}_{27}\text{H}_{20}\text{N}_4\text{FeF}_4$: C, 60.92 (60.66); H, 3.79 (2.53); N, 10.52 (10.21). Infrared (Nujol): $\nu(\text{CN}) = 2175\text{m}$ and 2194s cm^{-1} .

The following compounds were prepared analogously.

$[\text{FeCpCp}^*]^+[\text{C}_4(\text{CN})_6]^-$. Anal. Calcd (found) for $\text{C}_{25}\text{H}_{20}\text{FeN}_6$: C, 65.23 (64.96); H, 4.38 (3.83); N, 18.26 (18.36). Infrared (Nujol): $\nu(\text{CN}) = 2190\text{s}$, 2222w , and 2247w cm^{-1} .

$[\text{FeCpCp}^*]^+[\text{DDQ}]^-$. Anal. Calcd (found) for $\text{C}_{23}\text{H}_{20}\text{Cl}_2\text{FeN}_2\text{O}_2$: C, 57.17 (56.89); H, 4.17 (3.97); N, 5.80 (5.57). Infrared (Nujol): $\nu(\text{CN}) = 2209\text{s cm}^{-1}$.

$\{[\text{FeCpCp}^*]^+[\text{TCNQ}]^-\}_2$. Anal. Calcd (found) for $\text{C}_{39}\text{H}_{28}\text{FeN}_8$: C, 70.49 (70.55); H, 4.25 (3.88); N, 16.86 (16.67). Infrared (Nujol): $\nu(\text{CN}) = 2193\text{m}$ and 2202m cm^{-1} .

X-ray Data Collection, Reduction, Solution, and Refinement. The single-crystal X-ray structures of $[\text{FeCpCp}^*]^+[\text{TCNE}]^{\bullet-}$, $\{[\text{FeCpCp}^*]^+\}_2[\text{TCNE}]_2^{2-}\cdot 2\text{MeCN}$, and $\{[\text{FeCpCp}^*]^+\}_2[\text{TCNE}]_2^{2-}\cdot \text{TCNE}\cdot \text{S}$ ($\text{S} = \text{CH}_2\text{Cl}_2$, THF) were solved by standard techniques using the Patterson heavy-atom method, which yielded the position of the Fe atom. The remaining atoms were located in subsequent Fourier difference maps. A summary of the experimental conditions are presented in Table 1, while the remaining structural information is presented as Supporting Information.

Spectroscopic Measurements. Infrared spectra were recorded on a Nicolet 7199 Fourier transform spectrometer. The UV-visible spectra were recorded on a Cary 2390 spectrometer. The EPR spectra were recorded on an IBM/Bruker ER 200 D-SRC spectrometer in a mixture of CH_2Cl_2 and 3-methyltetrahydrofuran.

Magnetic Measurements. The magnetic susceptibility was determined for powder samples between 2.0 and 320 K and with a 5.2–19.5 kG applied field range using a Faraday balance at Du Pont as previously described.¹¹

Results and Discussion

To prepare additional examples of molecule-based magnets based on the electron-transfer salt of a metallocene and TCNE, in particular to maintain 5-fold symmetry to identify the structure–function relationship, the reaction between FeCpCp^* and TCNE as well as other acceptors, e.g., TCNQ, $\text{C}_4(\text{CN})_6$, TCNQF_4 , and DDQ, was investigated. The reaction of FeCpCp^* and TCNE in MeCN leads to the solvate $[\text{FeCpCp}^*][\text{TCNE}]\cdot \text{MeCN}$, analogous to the stoichiometry that was observed for $[\text{FeCp}_2][\text{TCNE}]\cdot \text{MeCN}$ ³ but different in structure (vide infra). Like $[\text{FeCp}_2][\text{TCNE}]\cdot \text{MeCN}$, $[\text{FeCpCp}^*][\text{TCNE}]\cdot \text{MeCN}$ readily lost solvent and became polycrystalline.³ Since the reaction of FeCp_2 and TCNE in THF and CH_2Cl_2 leads to crystals, albeit structurally disordered, of solvent-free $[\text{Fe}^{\text{III}}\text{Cp}_2]$ -

- (7) McConnell, H. M. *Proc. R. A. Welch Found. Chem. Res.* **1967**, *11*, 144. Miller, J. S.; Epstein, A. J. *J. Am. Chem. Soc.* **1987**, *109*, 3850.
 (8) Miller, J. S.; Glatzhofer, D. T.; O'Hare, D. M.; Reiff, W. M.; Chackraborty, A.; Epstein, A. J. *Inorg. Chem.* **1989**, *28*, 2930.
 (9) (a) Bunel, E. E.; Valle, L.; Manriquez, J. M. *Organometallics* **1984**, *3*, 1680. (b) Phillips, L.; Lacey, A. R.; Cooper, M. K. *J. Chem. Soc., Dalton Trans.* **1988**, 1383.
 (10) (a) Webster, O. J. *Am. Chem. Soc.* **1964**, *86*, 2898. (b) Wheland, R. C.; Martin, E. L. *J. Org. Chem.* **1975**, *40*, 1301.

- (11) Miller, J. S.; Dixon, D. A.; Calabrese, J. C.; Vazquez, C.; Krusic, P. J.; Ward, M. D.; Wasserman, E.; Harlow, R. D. *J. Am. Chem. Soc.* **1990**, *112*, 381.

Table 1. Summary of the Crystallographic Details for [FeCpCp*][TCNE], [FeCpCp*][TCNE]·MeCN, [FeCpCp*]₂[TCNE]₃·THF, and [FeCpCp*]₂[TCNE]₃·CH₂Cl₂

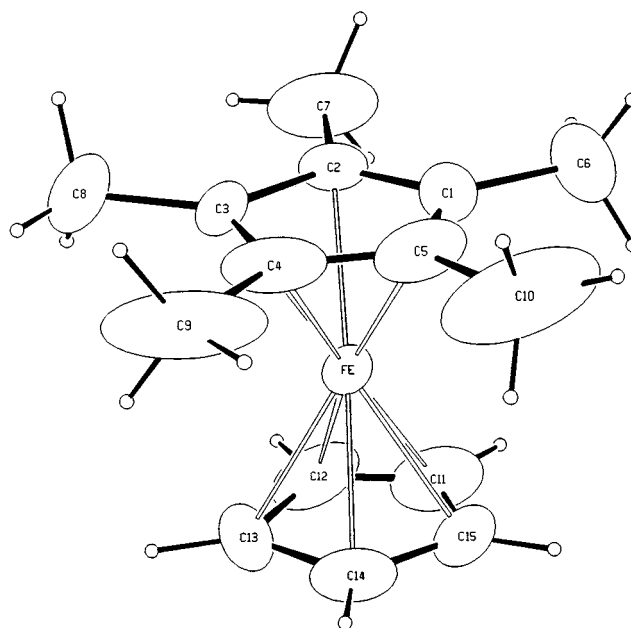
	[FeCpCp*] ₂ [TCNE] ₃ ·CH ₂ Cl ₂	[FeCpCp*] ₂ [TCNE] ₃ ·THF	[FeCpCp*][TCNE]	[FeCpCp*][TCNE]·MeCN
TCNE/Fe ratio	1.5	1.5	1.0	1.0
formula	C ₄₉ H ₄₂ Cl ₂ N ₁₂ Fe ₂	C ₅₂ H ₄₈ N ₁₂ Fe ₂ O	C ₂₁ H ₂₀ N ₄ Fe	C ₂₅ H ₂₆ N ₆ Fe
fw	981.57	968.73	384.27	425.32
space group	P2 ₁ /c (No. 14)	C2/c (No. 15)	P2 ₁ /m (No. 11)	P2 ₁ /n (No. 14)
a, Å	12.654(3)	12.985(7)	8.349(5)	8.826(2)
b, Å	22.254(7)	22.829(3)	13.338(3)	17.603(2)
c, Å	16.919(4)	17.050(4)	10.253(5)	13.900(3)
β, deg	91.24(2)	90.27(3)	111.47(2)	90.64(1)
V, Å ³	4763.3	5054	1062.5	2159.4
λ, Å	0.710 73	0.710 73	0.710 73	0.710 73
Z	4	4	2	4
ρ(calcd), g/cm ³	1.368	1.27	1.201	1.308
abs coeff, cm ⁻¹	7.68	6.2	7.17	7.13
temp, °C	-100	23	-65	-70
R ^a	0.057	0.074	0.084	0.038
R _w ^b	0.045	0.093	0.079	0.037

$$^a R = \sum(|F_o| - |F_c|) / \sum|F_o|. \quad ^b R_w = [\sum w(|F_o| - |F_c|)^2 / \sum w|F_o|^2]^{1/2}.$$

[TCNE]₃·Fe^{II}CpCp* and TCNE were reacted in these solvents to obtain a solvent-free material. However, unprecedentedly, materials of [FeCpCp*]₂[TCNE]₃·S (S = THF, CH₂Cl₂) composition were isolated and structurally, spectroscopically, and magnetically characterized. Fortunately, albeit on one occasion, crystals of solvent-free [FeCpCp*][TCNE] were isolated and characterized. The infrared ν_{C≡N} absorptions for the [TCNE]^{•-} salts are more complex with absorptions at 2144 and 2183 cm⁻¹, characteristic of isolated [TCNE]^{•-} for solvent-free [FeCpCp*][TCNE], and at 2161, 2174, and 2191 cm⁻¹ for [FeCpCp*]₂[TCNE]₃·S and [FeCpCp*][TCNE]·MeCN. This three-band pattern is characteristic of [TCNE]₂²⁻ dimers.¹² Additionally, [FeCpCp*]₂[TCNE]₃·S have ν_{C≡N} absorptions at 2237 and 2263 cm⁻¹ attributed to TCNE⁰.^{13,14a} Hence, on the basis of the ν_{C≡N} IR spectral data, the following compounds were characterized: [Fe^{III}CpCp*]^{•+}[TCNE]^{•-}, {[Fe^{III}CpCp*]^{•+}}₂[TCNE]₂²⁻·2MeCN, {[Fe^{III}CpCp*]^{•+}}₂[TCNE]₂²⁻·TCNE⁰·S (S = THF, CH₂Cl₂).

Additionally, electron-transfer salts of FeCpCp* with TCNQ, C₄(CN)₆, TCNQF₄, and DDQ were prepared. These darkly colored materials exhibit ν_{C≡N} vibrational absorptions [i.e., 2209s cm⁻¹ for [DDQ]^{•-}, 2190s, 2222w, and 2247w cm⁻¹ for [C₄(CN)₆]^{•-} and 2175m and 2194s for [TCNQF₄]^{•-}].^{13,14a-c} and magnetic susceptibility data characteristic of the radical anion.

For the TCNQ product, the ν_{C≡N} of 2193 and 2202 cm⁻¹ are higher in frequency than those expected for [TCNQ]^{•-} (i.e., 2153 and 2179 cm⁻¹) and lower in frequency than those expected for TCNQ⁰ (i.e., 2222 and 2226 cm⁻¹)^{6b,13} and are typical of a delocalized 1-D chain comprising [TCNQ]^{1/2-}.¹⁵ FeCpCp*, like ferrocene, can only be isolated as a 1:2 electron-transfer complex with TCNQ. Undoubtedly, like [FeCp₂][TCNQ]₂^{16a} and [FeCp*]₂[TCNQ]₂,^{16b} [FeCpCp*][TCNQ]₂ is expected to be a semicon-

**Figure 1.** ORTEP plot (30%) of [FeCpCp*]^{•+} as observed in [FeCpCp*]^{•+}[TCNE]^{•-}. Similar structures are observed for {[FeCpCp*]^{•+}}₂[TCNE]₂²⁻·2MeCN and [FeCpCp*]₂[TCNE]₃·CH₂Cl₂.

ductor. Since crystals suitable for single-crystal X-ray diffraction could not be obtained; further studies on this material were curtailed.

The structures of [FeCpCp*][TCNE], {[FeCpCp*]^{•+}}₂[TCNE]₂²⁻·2MeCN, and [FeCpCp*]₂[TCNE]₃·S (S = THF, CH₂Cl₂) have been determined (Table 1). Each comprises [FeCpCp*]^{•+} cations as well as TCNE present as [TCNE]^{•-}, [TCNE]₂²⁻, or TCNE⁰.

Structure of [FeCpCp*]^{•+} Cations. Since the structures of the [FeCpCp*]^{•+} cations are comparable, they will be discussed together, and because of the differences between the anions, each anion as well as their packing motif will be discussed separately. The structures of [FeCpCp*]^{•+}[TCNE]^{•-} (Figure 1), {[FeCpCp*]^{•+}}₂[TCNE]₂²⁻·2MeCN, and [FeCpCp*]₂[TCNE]₃·CH₂Cl₂ have ordered D₅ [FeCpCp*]^{•+} cations with structural parameters essentially equivalent to those previously reported for [FeCp₂]^{•+} and [FeCp*]₂^{•+} (Table 2).^{3,4,6,13,14,18} For the Cp ring, the Fe—C and C—C distances average 2.079 and 1.385

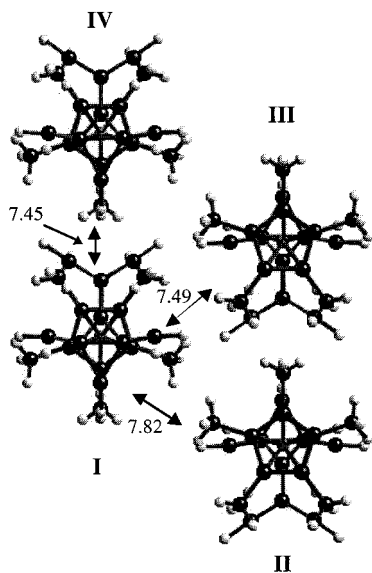
- (12) (a) Miller, J. S.; O'Hare, D. M.; Chakraborty, A.; Epstein, A. J. *J. Am. Chem. Soc.* **1989**, *111*, 7853. (b) Lemervoskii, D. A.; Stukan, R. A.; Tarasevich, B. N.; Slovokhotov, Yu. L.; Antipin, M. Yu.; Kalinin, A. E.; Struchov, Yu. T. *Struct. Khim.* **1981**, *7*, 240. (c) Novoa, J. J.; Lafuente, P.; Del Sesto, R. E.; Miller, J. S. Manuscript submitted.
- (13) Miller, J. S.; Dixon, D. A. *Science* **1987**, *235*, 871.
- (14) (a) Miller, J. S.; Krusic, P. J.; Dixon, D. A.; Reiff, W. M.; Zhang, J. H.; Anderson, E. C.; Epstein, A. J. *J. Am. Chem. Soc.* **1986**, *108*, 4459. (b) Dixon, D. A.; Calabrese, J. C.; Miller, J. S. *J. Phys. Chem.* **1991**, *95*, 3139. (c) Miller, J. S.; Zhang, J. H.; Reiff, W. M.; Preston, L. D.; Reis, A. H., Jr.; Gerbert, E.; Extine, M.; Troup, J.; Ward, M. D. *J. Phys. Chem.* **1987**, *91*, 4344. (d) Johnson, M. T.; Arif, A. M.; Miller, J. S. *Eur. J. Inorg. Chem.* **2000**, 178. Dixon, D. A.; Calabrese, J. C.; Miller, J. S. *J. Phys. Chem.* **1988**, *93*, 2284. (e) Dixon, D. A.; Miller, J. S. *J. Am. Chem. Soc.* **1987**, *109*, 3656.
- (15) Chappell, J. S.; Bloch, A. N.; Bryden, W. A.; Maxfield, M.; Poehler, T. O.; Cowan, D. *J. Am. Chem. Soc.* **1981**, *103*, 2442.

- (16) (a) Melby, L. R.; Harder, R. J.; Hertler, W. R.; Mahler, W.; Benson, R. E.; Mochel, W. E. *J. Am. Chem. Soc.* **1962**, *84*, 3374. (b) Miller, J. S.; Reis, A. H., Jr.; Candela, G. A. *Lect. Notes Phys.* **1979**, *96*, 313.

Table 2. Summary of Crystallographically Determined Bond Lengths for $[\text{FeCp}_2]^{II}$, $[\text{FeCp}^*_2]^{II}$, and $[\text{FeCpCp}^*]^{II}$

salt	Fe...C (Cp ring)	Fe...Cp centroid	Fe...C (Cp* ring)	Fe...Cp* centroid	ref
$\text{Fe}^{II}\text{Cp}_2$	2.108	1.656			4c
$[\text{Fe}^{III}\text{Cp}_2]^{II}$	2.07 ^b	1.70 ^b			3, 16a, 18
$\text{Fe}^{II}\text{CpCp}^*$	<i>a</i>	1.658	<i>a</i>	1.642	17b
$[\text{Fe}^{III}\text{CpCp}^*]^{II}$	2.079	1.712	2.081	1.692	this work
$\text{Fe}^{II}\text{Cp}^*_2$			2.050	1.656	17a
$[\text{Fe}^{III}\text{Cp}^*_2]^{II}$			2.09 ^b	1.70 ^b	3

^a Not reported. ^b Average value.

**Figure 2.** View normal to the parallel chains showing the key interchain distances (Å) between chains **I**, **II**, **III**, and **IV** for $[\text{FeCpCp}^*]^{II}[\text{TCNE}]^{2-}$.

Å, respectively. For the Cp* ring, the Fe–C, C–C, and C–Me separations average 2.081, 1.425, and 1.497 Å, respectively. The Fe–C₅ ring centroid distances are 1.712 Å (Cp) and 1.692 Å (Cp*). These centroids are 0.05 Å shorter than that for $\text{Fe}^{II}\text{CpCp}^*$,^{17b} and this trend is observed for FeCp_2 ,^{4c,16a,18} and FeCp^*_2 .^{3,17a} The *D*₅ cation in the structure of $[\text{Fe}(\text{C}_5\text{Me}_5)(\text{C}_5\text{H}_5)]_2[\text{TCNE}]_3\cdot\text{THF}$ is disordered, but the distances are comparable to those for the other three compounds.

Structures of $[\text{TCNE}]^{2-}$ Anions. $[\text{FeCpCp}^*]^{II}[\text{TCNE}]^{2-}$ comprises an anion that is disordered in at least two orientations across a mirror plane. Attempts to break the potential pseudomirror (i.e., *P*₂₁) were unsuccessful. The planar anion is disordered and does not warrant a discussion of its structure. Although the anions are disordered, the packing motif can be discerned and, like that observed for $[\text{FeCp}^*_2][\text{TCNE}]$,³ consists of parallel 1-D $\cdots\text{D}^+\text{A}^-\text{D}^+\text{A}^-\text{D}^+\text{A}^-\cdots$ chains that are separated by 7.45, 7.49, and 7.82 Å (Figure 2). There are three unique out-of-registry interchain interactions, namely, **I–II**, **I–III**, and **I–IV** (Figure 3), with interchain Fe...Fe separations of 8.133, 8.349, 8.977, 9.651, 10.591, and 10.782 Å. The intrachain Fe...Fe separation is 10.253 Å. The comparable distances in $[\text{FeCp}^*_2][\text{TCNE}]$ are 8.232 and 8.732 Å for the chain separations, which represent 9% shorter distances, while the interchain Fe...Fe separations of 9.473, 10.028, 10.212, and 13.591 Å are more than 16% greater than those for $[\text{FeCpCp}^*][\text{TCNE}]$. In contrast the 10.451 Å intrachain Fe...Fe separation³ is only 2% shorter.

Hence, these distances are all shorter than that observed for the $[\text{FeCp}^*_2][\text{TCNE}]$ as a consequence of the lower steric bulk of $[\text{Fe}^{III}\text{Cp}_2]^{II}$ with respect to $[\text{Fe}^{III}\text{Cp}^*_2]^{II}$. Thus, the shortened separation suggest stronger magnetic interactions.

$\{[\text{FeCpCp}^*]^{II}\}_2[\text{TCNE}]_2^{2-}\cdot 2\text{MeCN}$ has a planar 2-fold disordered anion and acetonitrile solvation. The bond distances and angles for the anion are given in Table 3. The 2-fold disorder of the anion was treated by refining the atom multiplicities with reasonable temperature factors. The disorder leads to a relatively poor structure with the central C–C bond being 1.388(10) Å while the NC–C and C≡N separations range from 1.402(8) to 1.541(9) and from 1.097(4) to 1.114(4) Å and average 1.47 and 1.106 Å, respectively. The $[\text{TCNE}]_2^{2-}$ dimer is structurally distinct from the eclipsed dimer previously reported (vide infra).¹² A cyano carbon lies directly under (2.98 Å) the center of the plane defined by the pair of ethylene carbons each at 50% occupancy. These planes are separated by 2.79 Å (Figure 4a). The unit cell consists of a herringbone array of $\text{SD}^+\text{A}_2^{2-}\text{D}^+\text{S}$ dimers separated by a solvent molecules (*S* = MeCN) (Figure 5).

Both 2:3 compounds, $[\text{FeCpCp}^*]_2[\text{TCNE}]_3\cdot\text{S}$ (*S* = THF, CH₂Cl₂), contain $[\text{TCNE}]_2^{2-}$ dimer dianions as well as a neutral molecule of TCNE (Figure 4b,c). The structures of the two compounds are similar, with more disorder being present in the THF compound. The structure of the CH₂Cl₂ compound is illustrated in Figure 6. The central C–C bond distances are 1.321 Å (THF) and 1.347 Å (CH₂Cl₂) for $[\text{TCNE}]^0$ and 1.372 Å (THF) and 1.459 Å (CH₂Cl₂) for the dianion, consistent with bond orders of 2 and 1.5, respectively. The central C–C bonds are eclipsed in the centrosymmetric $[\text{TCNE}]_2^{2-}$ dimer and are separated by 2.903 Å (THF) and 2.833 Å (CH₂Cl₂). Each monomer in the *S* = 0 $[\text{TCNE}]_2^{2-}$ dimer is not planar, but bent 5.75° (THF) and 6.45° (CH₂Cl₂) out of the formal TCNE plane via a *b*₃₀ out-of-plane vibration. Similar $[\text{TCNE}]_2^{2-}$ dimers with a similar intradimer separation of 2.90 Å and out-of-plane bending of the CN by 5.6° have also been observed for the electron-transfer salts $[\text{Fe}(\text{C}_5\text{H}_4)_2(\text{CH}_2)_3][\text{TCNE}]^{12b}$ and $[\text{Cr}(\text{C}_6\text{Me}_{6-x}\text{H}_{x-3})_2][\text{TCNE}]$ (*x* = 3, 6).^{12a}

$[\text{FeCpCp}^*]_2[\text{TCNE}]_3\cdot\text{S}$ (*S* = CH₂Cl₂, THF) also possess two $[\text{FeCpCp}^*]^{II}$ cations in the asymmetric unit (Figure 6). In the CH₂Cl₂ solvate, the Fe...Fe distance between the cations is 7.089 Å and the closest C...C distance between the Cp rings is 3.334 Å. In the THF solvate, the cations are farther apart, with an Fe...Fe distance of 7.362 Å and the closest C_{Cp}...C_{Cp} distance of 3.776 Å. Although the cations are distant from each other, interpretation of the magnetic data suggests some weak singlet–triplet interactions for the CH₂Cl₂ solvate (vide infra) but not for the THF solvate.

EPR. EPR spectra of ferrocenium ions are only observable in dilute diamagnetic glasses at liquid helium temperatures.^{19a,b} The *d*⁵ *a*_{1g}²*e*_g³ electronic configuration of ferrocenium cations results in a ²E_{2g} ground state in *D*₅ point symmetry. The ²E ground state allows for rapid spin–lattice relaxation and highly anisotropic *g* tensors. Prins has derived approximate *g*-value expressions appropriate for ferrocenium cations:^{19a}

$$g_z = g_{||} = 2 + 4k_{||}[-(\xi/\delta)/(1 + \xi^2/\delta^2)^{1/2}]$$

$$g_x = g_y = g_{\perp} = 2/(1 + \xi^2/\delta^2)^{1/2}$$

where ξ is the spin–orbit coupling (ca. 328 cm⁻¹ for Fe³⁺ 19c),

(17) (a) Freyberg, D. P.; Robbins, J. L.; Raymond, K. N.; Smart, J. C. *J. Am. Chem. Soc.* **1971**, *93*, 892. (b) Bildstein, B.; Hradsky, A.; Kopacka, H.; Malleier, R.; Ongania, K.-H. *J. Organomet. Chem.* **1997**, *540*, 127.
(18) Miller, J. S.; Zhang, J. H.; Reiff, W. H. *Inorg. Chem.* **1987**, *26*, 600.

(19) (a) Warren, K. D. *Struct. Bonding* **1976**, *45*, 45. Prins, R. *Mol. Phys.* **1970**, *19*, 602. (b) Ammeter, J. H. *J. Magn. Res.* **1978**, *30*, 299. (c) Duggan, D. M.; Hendrickson, D. N. *Inorg. Chem.* **1975**, *14*, 955.

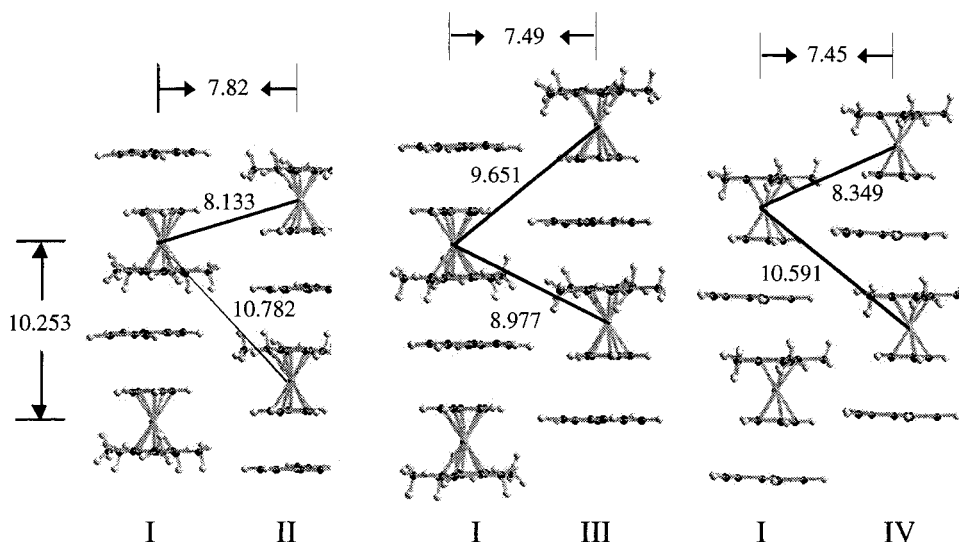


Figure 3. View parallel to out-of-registry chains I–II (a) and I–III (b), and in-registry chains I–IV (c) for $[\text{FeCpCp}^*]^{2+}[\text{TCNE}]^{2-}$. Distances are in angstroms.

Table 3. Summary of Crystallographically Determined Bond Lengths and Angles and $\nu_{\text{C}=\text{N}}$ for $[\text{TCNE}]_2^{2-}$

cation	$[\text{Fe}(\text{C}_5\text{H}_4)_2(\text{CH}_2)_3]_2^{2+}$	$[\text{Cr}(\text{C}_6\text{H}_6)_2]^{2+}$	$[\text{FeCpCp}^*]^{2+ a}$		
solvent			MeCN	CH_2Cl_2	THF
temp, °C	–120	23	–70	–100	23
C–C, Å	1.35 (2)	1.436	1.406	1.459	1.372
C–CN, Å	1.46	1.408	<i>c</i>	1.417	1.448
C≡N, Å	1.13	1.139	1.106	1.132	1.110
C–C≡N, deg	175.0	178.4	<i>c</i>	177.2	175.1
NC–C–CN, deg	118.5	118.6	<i>c</i>	118.0	119.7
C–C–CN, deg	120	120.2	<i>c</i>	120.5	119.7
deviation out of plane, deg ^b	5.5	6.0	<i>c</i>	6.45	5.75
<i>R</i> _w , %	13.1	4.4	3.7	4.5	9.3
dimer separation, Å	2.90	2.90	2.79	2.833	2.903
$\nu_{\text{C}=\text{N}}$, cm ^{–1}	2161	2159	2163	2160	2159
	2168	2170	2175	2173	2173
	2191	2189	2192	2190	2190
ref	12b	12a	this work	this work	this work

^a $[\text{FeCpCp}^*]_2^{2+}[\text{TCNE}]_2^{2-} \cdot \text{TCNE} \cdot \text{S}$ ^b Calculated from half of the average trans NC···CN dihedral angles using CrystalMaker4. ^c Unable to determine because of disorder.

k_{\parallel} is the orbital reduction factor, and δ is the one-electron orbital energy splitting that scales the distortion from D_5 symmetry.¹⁹

The g values for ferrocenium cations are generally very far from the free-electron g value because they are dominated by contributions from orbital angular momentum.¹⁹ However, for ferrocenium systems with lower symmetry and a larger distortion parameter δ , the g -tensor anisotropy Δg ($\Delta g = g_{\parallel} - g_{\perp}$) decreases and approaches 2.0. Thus, EPR is an important probe for the distortions of ^2E ground states.

The EPR spectrum of $[\text{FeCpCp}^*]^{2+}[\text{BF}_4]^{-}$ at 5 K shows an axially symmetrical powder pattern characterized by $g_{\parallel} = 4.36$ and $g_{\perp} = 1.24$. Like $[\text{FeCp}_2]^{2+}$ and $[\text{FeCp}^*_2]^{2+}$ a spectrum is not observed at 77 K. These values are comparable to those reported for other ferrocene cations.^{8,19} The Δg of 3.12 is comparable to 3.08 ± 0.01 determined for both ferrocenium and decamethylferrocenium cations. This supports the assignment that $[\text{FeCpCp}^*]^{2+}$ is isoelectronic with these cations and has a $^2\text{E}_{2g}$ ground state.

The one-electron orbital energy splitting, δ , varies extensively and is strongly dependent on the degree of substitution. The k_{\parallel} parameter, which reflects the extent of metal–ligand mixing and the strength of the vibronic coupling, is small. Nonetheless, δ for $[\text{FeCpCp}^*]^{2+}$ is 259 cm^{-1} , which is in good agreement with the values for $[\text{Fe}(\text{C}_5\text{Me}_4\text{H})_2]^{2+}$ (338 cm^{-1}),⁷ $[\text{FeCp}^*_2]^{2+}$ (301 cm^{-1}), and $[\text{FeCp}_2]^{2+}$ (266 cm^{-1}),¹⁹ suggesting that the

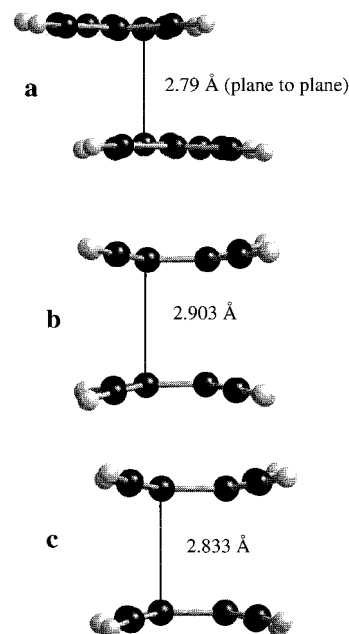


Figure 4. Structure of $[\text{TCNE}]_2^{2-}$ present in (a) $[\text{FeCpCp}^*]^{2+}[\text{TCNE}]^{2-} \cdot \text{MeCN}$, (b) $[\text{FeCpCp}^*]_2[\text{TCNE}]_3 \cdot \text{THF}$, and (c) $[\text{FeCpCp}^*]_2[\text{TCNE}]_3 \cdot \text{CH}_2\text{Cl}_2$. Distances are in angstroms.

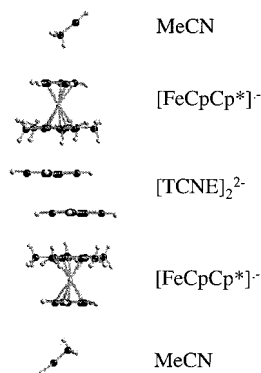


Figure 5. Structure of the repeat unit in $[\text{FeCpCp}^*]^+[\text{TCNE}]^{2-} \cdot \text{MeCN}$.

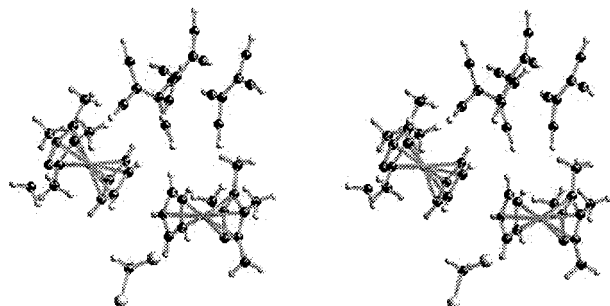


Figure 6. Stereoview of the formula unit of $[\text{FeCpCp}^*]_2[\text{TCNE}]_3 \cdot \text{CH}_2\text{Cl}_2$.

Table 4. Effective Moment and Weiss Constant for $[\text{FeCpCp}^*][\text{A}]$ Electron-Transfer Salts

anion, A	$\mu_{\text{eff}}/\text{Fe}, \mu_{\text{B}}/\text{Fe}$	θ, K
$[\text{BF}_4]^-$	3.34	+1.8
$[\text{TCNE}]^{1-} (1:1)^a$	3.43	+3.3
$[\text{TCNE}]_2^{2-} (1:1)^b$	2.08	-1.6
$[\text{TCNE}]_2^{2-} (2:3)^c$	3.31	-2.0 ^e
$[\text{TCNE}]_2^{2-} (2:3)^d$	3.04	0.0
$[\text{TCNQF}_4]^{2-}, T > 220 \text{ K}$	3.35	-1.5 ^e
$[\text{C}_4(\text{CN})_6]^{4-}$	2.76	-1.1
$[\text{TCNQ}]^{1/2-} (1:2), T > 70 \text{ K}$	2.99	-32
$T < 70 \text{ K}$	2.55	-1.9
$[\text{DDQ}]^{1-}$	2.56	-1.3

^a Nonsolvated, average of three samples. ^b Contains MeCN. ^c Contains CH_2Cl_2 . ^d Contains THF. ^e Fit to eq 1.

separation arising from the splitting of the e_g orbital imposed by the C_{2h} symmetry is small.

Magnetic Susceptibility. The 2–320 K Faraday balance magnetic susceptibility of the $[\text{FeCpCp}^*]^+$ salts can be fit by the Curie–Weiss expression, $\chi \propto (T - \theta)^{-1}$. The effective moment, $\mu_{\text{eff}} [= (8\chi T)^{1/2}]$, and θ values are listed in Table 4. The effective moment for a polycrystalline sample of $[\text{FeCpCp}^*]^+[\text{BF}_4]^-$ is $3.34 \mu_{\text{B}}$, and θ is 1.8 K. The small positive Weiss constant, θ , is consistent with that observed for $[\text{Fe}(\text{C}_5\text{Me}_4\text{H})_2]^+[\text{BF}_4]^-$ ($\theta = 1.6 \text{ K}$)⁸ and suggests a small amount of ferromagnetic coupling. The moment is much greater than expected from a randomly oriented sample based on $\langle g \rangle$ (i.e., $2.34 \mu_{\text{B}}$ for $\langle g \rangle = 2.71$) but is less than expected for a sample oriented with the C_5 axis parallel to the magnetic field (i.e., $3.78 \mu_{\text{B}}$ for $g_{\parallel} = 4.36$) and substantially greater than that expected for a sample oriented with the C_5 axis perpendicular to the magnetic field (i.e., $1.07 \mu_{\text{B}}$ for $g_{\perp} = 1.24$). These values are typical of $[\text{FeCp}_2]^+$ and $[\text{FeCp}^*]_2^+$ salts with diamagnetic anions.^{7,8,19}

Similar effective moments (2.08–3.43 μ_{B}/Fe) are obtained for the $[\text{TCNE}]^{1-}$, $[\text{C}_4(\text{CN})_6]^{4-}$, $[\text{TCNQ}]^{1-}$, $[\text{TCNQF}_4]^{1-}$, and

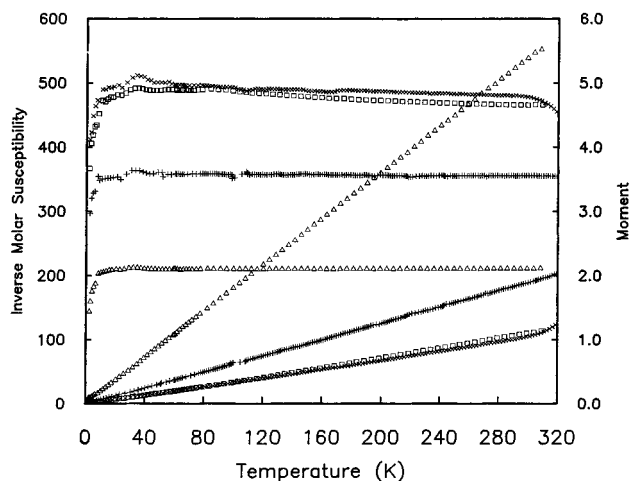


Figure 7. Temperature dependencies of the reciprocal molar magnetic susceptibility, χ^{-1} , and effective moment, μ_{eff} , of $[\text{FeCpCp}^*][\text{TCNE}]$ (+), $[\text{FeCpCp}^*][\text{TCNE}] \cdot \text{MeCN}$ (Δ), $[\text{FeCpCp}^*]_2[\text{TCNE}]_3 \cdot \text{CH}_2\text{Cl}_2$ (\square), and $[\text{FeCpCp}^*]_2[\text{TCNE}]_3 \cdot \text{THF}$ (\times).

$[\text{DDQ}]^{1-}$ salts (Table 4). Thus, because of the orientation variability of polycrystalline samples, the observed effective moments are consistent for either one or two $S = 1/2$ radical(s) per formula unit, with one being $[\text{FeCpCp}^*]^+$. For most of these electron-transfer salts, the Curie–Weiss θ values are small, suggestive of very weak magnetic interactions.

As anticipated the 1-D phase of $[\text{FeCpCp}^*]^+[\text{TCNE}]^{1-}$ exhibits the largest moment ($3.43 \pm 0.10 \mu_{\text{B}}/\text{Fe}$) and a θ value of $+3.3 \pm 2.0 \text{ K}$; thus, as expected, this salt exhibits ferromagnetic coupling. The coupling, however, is weak with respect to the 30 K θ for the similarly structured $[\text{FeCp}^*]_2^+[\text{TCNE}]^{2-}$.^{2,3} Furthermore, unlike $[\text{FeCp}^*]_2[\text{TCNE}]$,³ magnetic ordering is not observed above 2 K. The similar structure with shorter interchain and intrachain out-of-registry distances that stabilize ferromagnetic coupling^{2,3,7} as well as the lack of in-registry separations that stabilize antiferromagnetic coupling^{2,3,7} is in opposition to the expectation of stronger ferromagnetic coupling as determined from the Weiss constant (θ), and ferromagnetic ordering at an enhanced critical temperature (T_c). Nonetheless, weaker ferromagnetic coupling is evident and magnetic ordering is not observed, and although the microscopic interactions that dominate are unclear, each of the 1-D chains has a net dipole moment, and interchain interactions with the same dipole moment as well as opposite dipole moments are present (Figure 3).

The detailed interpretation of the susceptibility due to the structural and vibrational characterization of the $[\text{FeCpCp}^*]_2[\text{TCNE}]_3 \cdot \text{S}$ ($\text{S} = \text{THF}, \text{CH}_2\text{Cl}_2$) can be made. TCNE exists as both the $S = 0$ TCNE^0 and $S = 0$ $[\text{TCNE}]_2^{2-}$; thus, only the spins from the cation contributes to the susceptibility. The observed moments of 3.04 ($\text{S} = \text{THF}$) and 3.31 ($\text{S} = \text{CH}_2\text{Cl}_2$) $\mu_{\text{B}}/\text{Fe}^{\text{III}}$ lie between the expected isotropic moment of $2.30 \mu_{\text{B}}/\text{Fe}^{\text{III}}$ and the fully aligned parallel to the chain direction moment of $3.69 \mu_{\text{B}}/\text{Fe}^{\text{III}}$ and indicate that the sample has some nonaverage orientation in the magnetic field. However, the reciprocal susceptibility, $\chi^{-1}(T)$, deviates from the Curie–Weiss law for both compounds. For $[\text{FeCpCp}^*]_2[\text{TCNE}]_3 \cdot \text{THF}$ the deviation occurs above $\sim 300 \text{ K}$ (Figure 7) and is attributed to sublimation of the complex. Thus, the magnetic susceptibility is consistent with the TCNE charge assignments. The plot of $\chi^{-1}(T)$ for $[\text{FeCpCp}^*]_2[\text{TCNE}]_3 \cdot \text{CH}_2\text{Cl}_2$ exhibits a change in slope at 80 K, below which θ is -1.4 K , while for $T > 80 \text{ K}$ θ is 14.8 K.

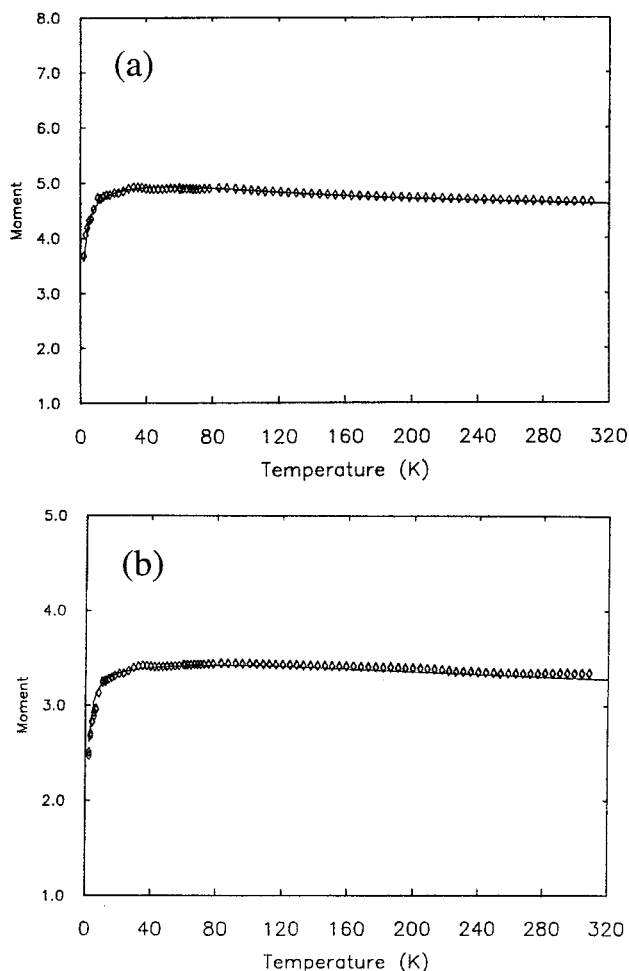


Figure 8. Temperature dependencies effective moment, μ_{eff} , of (a) $[\text{FeCpCp}^*]_2[\text{TCNE}]_3 \cdot \text{CH}_2\text{Cl}_2$ and (b) $[\text{FeCpCp}^*][\text{TCNQF}_4]$ and their fits to eq 1.

However, a more accurate model was also used (vide infra).

The $\mu_{\text{eff}}(T)$ data for both $[\text{FeCpCp}^*]_2[\text{TCNE}]_3 \cdot \text{CH}_2\text{Cl}_2$ and $[\text{FeCpCp}^*][\text{TCNQF}_4]$ rises slightly with decreasing temperature and after reaching a maximum at ca. 40 K decreases with decreasing temperature (Figure 8) and cannot be fit by the Curie–Weiss equation over the entire temperature range. Given that the TCNE anions are diamagnetic because of formation of $[\text{TCNE}]_2^{2-}$ dimers in the structure of $[\text{FeCpCp}^*]_2[\text{TCNE}]_3 \cdot \text{CH}_2\text{Cl}_2$ and that TCNQF_4 anions form diamagnetic $[\text{TCNQF}_4]_2^{2-}$ dimers unless N's can bond to a metal atom,^{6b,18} the magnetic behavior is solely attributed to the cations. The inability to fit $\mu_{\text{eff}}(T)$ with the Curie–Weiss equation is perplexing. Similar $\mu_{\text{eff}}(T)$ data were observed for $[[\text{Fe}(\text{C}_5\text{Me}_5)_2]^{+2}[\text{TCNQF}_4]^{2-}]$, which could be modeled by the Bleaney–Bowers equation arising from $S = 1/2$ cation–cation separations,²⁰

$$\chi = \frac{2Ng^2\mu_B^2}{k_B(T - \theta)[3 + e^{-2J/(k_B T)}]} \quad (1)$$

where N is Avogadro's number, g is the g value, μ_B is the Bohr magneton, and k_B is Boltzmann's constant.²¹ Hence, assuming some interaction between cations, the $\mu_{\text{eff}}(T)$ data were modeled by eq 1 above 2 K with $J/k_B = 175$ K (122 cm^{-1}), $\langle g \rangle = 3.56$,

and $\theta = -2.0$ K for $[\text{FeCpCp}^*]_2[\text{TCNE}]_3 \cdot \text{CH}_2\text{Cl}_2$ and with $J/k_B = 350$ K (243 cm^{-1}), $\langle g \rangle = 2.44$, and $\theta = -1.5$ K for $[\text{FeCpCp}^*][\text{TCNQF}_4]$ (Figure 8).

These $\langle g \rangle$ fall in the range of g_{\parallel} and g_{\perp} and indicate the samples are not randomly oriented. The positive J values indicate ferromagnetic coupling between the $[\text{FeCpCp}^*]^{+2}$ in these compounds, with stronger coupling associated with $[\text{FeCpCp}^*][\text{TCNQF}_4]$. The stronger coupling suggests shorter intercation interactions, but because the structure of $[\text{FeCpCp}^*][\text{TCNQF}_4]$ could not be determined, this could not be confirmed. The small negative θ values indicate weak antiferromagnetic coupling between the dimers.

$[\text{FeCpCp}^*][\text{TCNQ}]_2$ is anomalous as a change in slope of $\chi^{-1}(T)$ is evident at ~ 70 K. Above 70 K the reciprocal magnetic susceptibility obeys the Curie–Weiss expression with μ_{eff} of $2.99 \mu_B$ and $\theta = -32$ K, whereas below 70 K, $\mu_{\text{eff}} = 2.55 \mu_B$ and $\theta = -1.9$ K. The low-temperature values are comparable to the other $[\text{FeCpCp}^*]^{+2}$ salts; however, the high-temperature values suggest a higher moment state with substantial antiferromagnetic coupling. The susceptibility can be fit to a random exchange Heisenberg antiferromagnetic coupling (REHAC) model,²² i.e., $\chi \propto T^{-\alpha}$, with an exponent α of 0.85. The REHAC model predicts a sub-Curie dependence with $\alpha \approx 0.8$. The value of 0.85 suggests that this model may be applicable; however, because of the lack of structural information, detailed application and interpretation of the data with this model are unwarranted. This unusual magnetic behavior with respect to the other $[\text{FeCpCp}^*]^{+2}$ is attributed to the formation of a TCNQ-based conducting system as frequently occurs for 1:2 electron-transfer salts of TCNQ.²³ Crystallographic data should provide insight into this phenomenon, but the lack of suitable crystals has hampered continued studies in this area.

Conclusion

FeCpCp^* forms electron-transfer salts with strong electron acceptors. With TCNE, four materials were isolated that possessed $[\text{FeCpCp}^*]^{+2}$. The solvent-free salt $[\text{FeCpCp}^*]^{+2}[\text{TCNE}]^{2-}$, like that of $[\text{FeCp}^*]^{+2}$ and $[\text{Fe}(\text{C}_5\text{Me}_4\text{H})_2]^{+2}$, forms $\cdots \text{D}^{+2}\text{A}^{2-}\text{D}^{+2}\text{A}^{2-}\text{D}^{+2}\text{A}^{2-}\cdots$ 1-D chain structures and ferromagnetic coupling, but unexpectedly not ferromagnetic ordering as observed for related materials such as $[\text{FeCp}^*]^{+2}[\text{TCNE}]^{2-}$ ³ and $[\text{FeCp}^*]^{+2}[\text{TCNQ}]^{2-}$.⁶ The three solvated phases with TCNE possess diamagnetic $[\text{TCNE}]_2^{2-}$. The solvent has a dramatic effect on the formation of various structure types. Compounds with TCNE^0 , $[\text{TCNE}]^{2-}$, and/or $[\text{TCNE}]_2^{2-}$ have been isolated, illustrating that simple 1-D chain structures are not always favored. The formation of three different electron-transfer salts from FeCpCp^* and TCNE emphasizes the present inability to predict neither solid-state compositions nor structure types. The 1:1 1-D electron-transfer salt with TCNQ, however, could not be isolated.

Acknowledgment. We gratefully acknowledge support from the Department of Energy, Division of Materials Science, Grant Nos. DE FG 03-93ER45504 and DE FG 02-86BR45271 and the NSF Grant No. CHE-9730984.

Supporting Information Available: Tables of fractional coordinates/anisotropic thermal parameters, general temperature factors, and bond distances and angles for $[\text{FeCpCp}^*][\text{TCNE}]$, $[\text{FeCpCp}^*][\text{TCNE}] \cdot \text{MeCN}$, $[\text{FeCpCp}^*]_2[\text{TCNE}]_3 \cdot \text{S}$ ($\text{S} = \text{CH}_2\text{Cl}_2$, THF). This material is available free of charge via the Internet at <http://pubs.acs.org>.

IC0013983

(22) Sanny, J.; Clark, W. G. *Solid State Commun.* **1980**, *35*, 473. Ward, M. D.; Johnson, D. C. *Inorg. Chem.* **1987**, *26*, 4213.

(23) E.g.: Shibaeva, R. P.; Atovmyan, L. O. *Russ. Chem. Rev.* **1972**, *13*, 514.

(20) O'Hare, D.; Miller, J. S.; Zhang, J. H.; Reiff, W. H. Manuscript in preparation.

(21) Carlin, R. L. *Magnetochemistry*; Springer-Verlag: Berlin, 1986; p 88.